RSC Advances

ROYAL SOCIETY OF CHEMISTRY

www.rsc.org/advances

Nanoscale

RSCPublishing

ARTICLE

The art of the possible: computational design of the 1D and 2D materials based on the tetraoxa[8]circulene monomer

Cite this: DOI: 10.1039/x0xx00000x

Received ooth January 2014,
Accepted ooth January 2014

DOI: 10.1039/x0xx00000x

www.rsc.org/

G. V. Baryshnikov,*[a] B. F. Minaev[a,b], N. N. Karaush[a] and V.A. Minaeva[a]

The novel one- and two-dimensional π-conjugated materials containing tetraoxa[8]circulene monomer are designed on the basis of density functional theory techniques including the periodic boundary condition for the infinite structures. These new materials are predicted to be the perspective ambipolar organic semiconductors showing high mobility for hole and electron charge carriers. Furthermore, we demonstrate that the extention of π-conjugated tetraoxa[8]circulene units in the second dimension leads to the material with the HOMO-LUMO gap being significantly smaller than that for the 1D polymer ribbon. This fact clearly indicates the fundamental difference between the designed 1D and 2D semiconducting polymers which constitute the essence of modern "band-gap engineering". The consistent growth of π-conjugation determines the strong visible light absorption of the studied systems in a great contrast to the initial colorless of the tetraoxa[8]circulene compound. The possible chemical routs to synthesize the predicted materials are discussed including free Gibbs energy estimation for the proposed reactions.

Introduction

One of the main goals of molecular organic electronics is a controlled assembly of polymers, olygomers, molecular blocks or just small organic molecules into the desired architecture of the particular device providing simultaneously an efficient intermolecular electron and hole transport (or photonic parameters) and a high stability of the whole networks on a surface tightly bound by covalent interactions.[1] After discovery of conductivity in conjugated polymers the latter find various applications as semiconducting and luminescent materials in OLEDs and other optoelectronic devices.[2] The conjugated polymers and carbon nanotubes being one-dimensional (1D) assembly dominate now the field of organic electronics.

At the same time the two-dimensional (2D) materials such as graphene[3] and graphene-like[4] compounds are also attracting great attention in organic electronics especially in connection with various edges modifications[5] and patternization with regular pores in the graphene sheets[6]. The vanishing band gap between the valence and conduction zones in graphene provides a great shortcoming[7] for most optoelectronic device applications of this fantastic material.

Thus, the proper manipulating the structural arrangement of the 2D aggregates is very important for practical applications.[8] Manipulation with the regular pores[6] arrangement has recently been achieved in a graphene sheet; this success can open not only the energy band gap but also other possibilities which provide methods for introducing atoms, molecules, and functional groups into the regular pores for further functionalization.[6a]

Any production of the 2D graphene-like structures starting from macro solids of a graphite type can be classified as an assembly "from the top".[9] In the past decade, self-assembly on surfaces by supramolecular coordination has provided an approach for the "bottom-up" fabrication of 2D nanostructures[10].

A large network is difficult to create by traditional chemical synthesis, and especially it is not easy to deposit it on a surface while remaining intact[10a] since such assembly is typically very reactive and unstable.[5] It is known that the scanning tunneling microscope (STM) can be used to create covalent bonds between single molecules on a surface[1c], but this method is not suitable for applications in molecular electronics where a large number of molecules need to be connected in a desired device architecture.[1b,10a] Nowadays many laboratories try to use an ability of molecules to form supramolecular structures on nobel surfaces under high vacuum by self-assembly and create the tailor-made organic materials for molecular electronics.[10]

A great progress in organic chemistry on the surface now leads to the synthesis of planar 2D polymers.[8,10d,e] During last few years, the self-assembly on noble surfaces by supramolecular coordination have provided an efficient approach for the "bottom-up" fabrication of two-dimensional nanostructures (Fig. 1 b–e).[10] Y. Li et al[11] have recently studied the coordination self-assembly and metalation reaction of copper with 5,10,15,20-tetra(4-pyridyl)porphyrin (2HTPyP, Fig. 1c) on Au(111) surface. The porphyrin 2HTPyP is found to interact with copper through both the peripheral pyridyl groups and the porphyrin core. The first most easy polymerization occurs at room temperature when pairs of pyridyl groups from the neighboring molecules coordinate Cu(0) atoms; this leads to formation of a supramolecular metal-organic coordination network.[11] Annealing activates the intramolecular redox reaction, by which the coordinated copper atoms are oxidized to Cu(II) ions and the complexes Cu(II)TPyP are formed.[11] Above 520 K, the network degrades and the Cu(0) atoms in the linking positions are going out, while the Cu(II)TPyP complexes produce a close-packed

structure that is stabilized by the weak intermolecular interactions forming the two-dimensional coordination network.[11] Another way to produce the 2D porphyrin networks was recently realized by the stepwise polymerization of tetraphenylporphyrin (TPP) monomers with the different halogen-phenyl side groups (this process known as "hierarchical growth").[4a,8c,10a,b,12] The structure of produced polymers is very sensitive to the number and type of halogen moieties.[10a] As an example, the monohalogen substituted tetraphenylporphyrins can grow only in the single direction producing the corresponding dimers. Doubly halogenated TPPs are susceptible to the aligned coupling resulting in the 1D polymer (Fig. 1a). Finally, the tetrahalogen substituted TPPs are successfully extended into the second dimension producing the 2D networks (Fig. 2b).

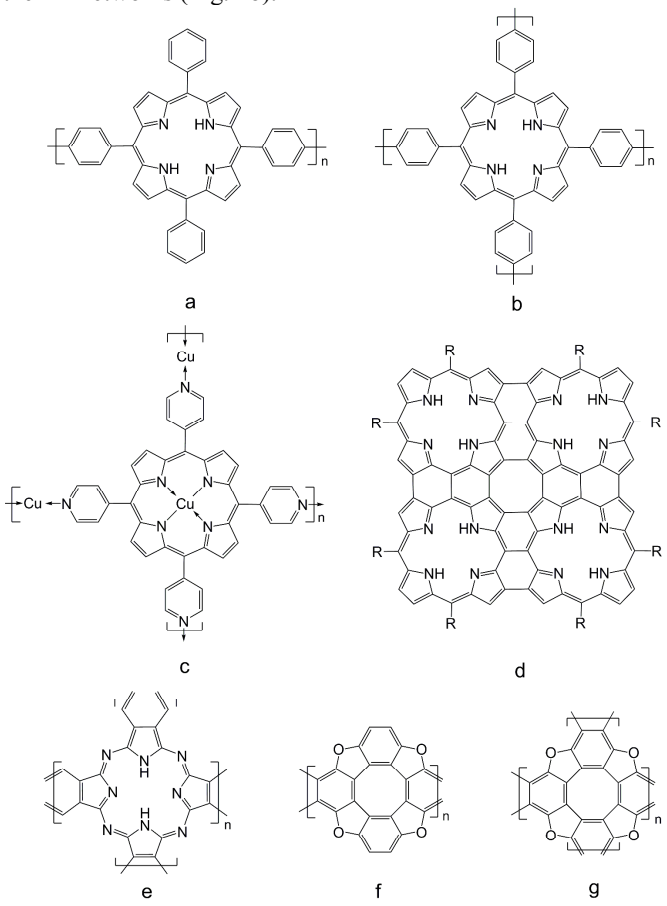

Fig. 1. Some examples of the 1D and 2D polimers containing porphyrin (a–d), phthalocyanine (e) and tetraoxa[8]circulene (f,g) monomers

The well-ordered organometallic sheets consisting of two-dimensional polymeric phthalocyanine moieties (Fig. 1e) represent another type of 2D polymers synthesized from the initial benzene-1,2,4,5-tetracarbonitrile according to the "bottom-up" principle.[13] E. Spitler and W. Dichtel[14] propose another way to obtain the phthalocyanine covalent organic frameworks by the $BF_3{\cdot}OEt_2$-catalysed 1,4-phenylenebis(boronic acid) esterification with the phthalocyanine tetra(acetonide). The synthetic availability, structural precision and robust nature of these materials make them perspective candidates for organic photovoltaic devices.

One more chemical rout to create the 2D π-conjugated materials by the "bottom-up" strategy is the direct *meso-meso* coupling of porphyrin subunits.[15] This reaction provides the formation of a non-planar cyclic porphyrin tetramer which is transformed into the planar porphyrin sheet (Fig. 1d) upon the subsequent oxidation process. By the same principle the linear 1D fused triple porphyrins were synthesized with the aim to create potential photonic wires.[16] These compounds demonstrate the particular spectral and electrochemical properties associated with the presence of strongly delocalized π-electronic system as a consequence of their planar structure.

In this way the porphyrin and phthalocyanine molecules are found to be the most promising building blocks to synthesize the novel 1D and 2D semiconducting materials (Fig. 1 a–e). In the present paper we want to propose another π-conjugated macrocyclic species, tetraoxa[8]circulene (TOC),[17] as a perfect candidate for 1D and 2D assembly (Fig. 1 f,g). This is because the TOC molecules are stable enough and synthetically available being susceptible well to peripheral functionality in both dimensions[18] due to the "square-planar" D_{4h} symmetry point group (like the metal porphyrins and phthalocyanines).

Computational methods

To investigate the structure, UV-visible absorption spectra, and charge carrier mobilities of new TOC-based materials a series of model compounds has been designed. One-dimensional oligomers (Fig. 1f) are constructed as n-repeating units along the 1D direction (n = 2–4, 9 and 16). The 2D sheets **1–3** were built as the square compounds sized by $\sqrt{n}\times\sqrt{n}$ (n = 4, 9, 16 for compounds **1**, **2**, **3**, respectively, Fig. 2). Another 2D sheet **4** was built asymmetrically in the form of a rectangle containing eight TOC units (Fig. 2). Terminal carbon atoms for all model compounds were closed with hydrogen. This building principle leads to the planar π-extended 2D sheets of the repeated monomers with four nearest neighbors each (Fig. 1g, excepting the terminal edge units).

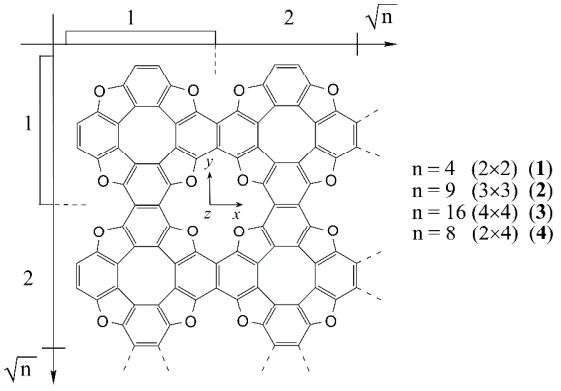

Fig. 2. The structure of the tetraoxa[8]circulene sheets (n denotes the total numbers of tetraoxa[8]circulene units, whereas $\sqrt{n}$ indicates the size of the corresponding square sheets, except rectangle compound **4**).

The equilibrium structural parameters of the studied molecules were optimized at the B3LYP/6-21G(d) level of the density functional theory (DFT)[19] with a control of possible symmetry constraints, using the Gaussian 09 software package[20] (there is no significant differences observed between the structural parameters, HOMO-LUMO gaps and charge carrier reorganization energies calculated with the 6-21G(d)

and extended 6-31G(d)[19d] basis sets for the low-mass oligomers containing up to nine TOC units). We have also calculated the Hessians for the 1D oligomers (n = 1–4) and for the simplest 2D square sheet structure conaining four TOC units (2 × 2, Fig. 2) with the same B3LYP/6-21G(d) method to determine vibrational frequencies and the true minimum of the total energy. All vibrational wavenumbers are found to be real, which indicates the location of the true minimum on the hypersurface of the total energy of the molecule. The electronic absorption spectra of all studied molecules are calculated by the time dependent (TD) DFT method[21] in gas phase using the same B3LYP functional and 3-21G basis set.

Reorganization energy values for the electron (λ_-) and hole (λ_+) carriers are calculated using the following equation widely used for estimation of the charge transport nature (n- or p-type conductivity) of organic materials:[22]

$$\lambda_{-/+} = (E^{*}_{-/+} - E_{-/+}) + (E^{**}_{-/+} - E_0)\,, \qquad (1)$$

where E_0 is the optimized ground state energy of the neutral molecule, $E_{-/+}$ is the optimized energy of the anionic/cationic molecule, $E^{**}_{-/+}$ is the energy of the neutral molecule at the anionic/cationic geometry and $E^{*}_{-/+}$ is the energy of the anionic/cationic molecule at the optimized geometry of the neutral species.

To estimate the magnetic properties of the designed materials the nucleus-independent chemical shift (NICS)[23] indexes are calculated for the simplest sheet **1** by the B3LYP/6-311++G(d,p) method (starting from the B3LYP/6-31G(d) optimized geometry) with the gauge-independent atomic orbital (GIAO) approximation.

All calculations are performed at the PDC supercomputers of the Royal Institute of Technology (Stockholm).

Results and discussion

Structural features. All designed compounds, including linear 1D oligomers and 2D sheets represent completely planar nanoscaled species. The square sheets **1–3** and the initial tetraoxa[8]circulene molecule correspond to the D_{4h} symmetry point group,[24] whereas linear oligomers and compound **4** are assigned to the D_{2h} symmetry. In the following discussion we shell focus on the structural features of 2D compounds **1–4**, which are the primary objects of the paper. The general size parameters (length, width and total area) of the designed sheets **1–4** (Fig. 2, 3) and ribbons (Fig. 1g) are presented in Table 1. As one can notice from the Table 1 the direct fusion of the TOC monomers along both dimensions provides the size decreasing of constructed sheets comparing with total size of the free initial TOC units. This is explained by the CH bonds disappearing upon condensation. (The data can be checked by the STM nano-size measurements and mass-spectra detection).

Table 1. Length (*a*), width (*b*) and total area (*S*) parameters for the TOC-based sheets **1–4** and 1D ribbons (n = 2–4, 9, 16).

Compound	*a*, nm	*b*, nm	*S*, nm^2	*M*, g mole^{-1}
1 ($C_{88}H_{16}O_{16}$)	1,86	1,86	3.46	1329.07
2 ($C_{192}H_{24}O_{36}$)	2.70	2.70	7.29	2906.27
3 ($C_{336}H_{32}O_{64}$)	3.54	3.54	12.53	5091.89
4 ($C_{172}H_{24}O_{32}$)	1.86	3.54	6.58	2602.05
1D ribbons ($C_{46}H_{12}O_8$ – $C_{354}H_{68}O_{64}$)	1.02	1.86 – 13.6	1.90 – 13.87	692.59–5344.37
TOC ($C_{24}H_8O_4$)	1.02	1.02	1.04	360.32

Now we shall analyze the structure of the simplest TOC-based sheet **1** in more detail including the T_1 exited state characterisation. One should note that compound **1** retains planar in the triplet excited state and corresponds to the D_{4h} symmetry point group like the ground singlet state. The T_1 state is higher in energy than the ground S_0 state by 2.11 eV, but the structure of the triplet sheet **1** is not significantly distorted comparing with the ground singlet state (Fig. S1). In both states the central cyclooctatetraene ring consists of the alternative short and long C–C bonds; but the average alternation difference ($\Delta\overline{R}$ ‡) between two neighbouring CC bonds is much higher for the S_1 state ($\Delta\overline{R}$ = 0.027 Å) than for the T_1 excited state ($\Delta\overline{R}$ = 0.017 Å). Such alternation parameter for both T_1 and S_0 states seems to be very weak in comparison with the hypothetical free planar cyclooctatetraene ($\Delta\overline{R}$ = 0.121 Å).[25] This fact qualitatively proves the very weak antiaromatic character of the inner eight-membered ring in **1–4** sheets compared with the strongly antiaromatic free planar cyclooctatetraene.[25]

A distinctive feature of the rectangle 2D sheets is that they become flexible and susceptible to the out-of plane bending upon the gradual growth. This phenomenon is well known as the "cochlea" model proposed by Kroto and McKay to describe the mechanism of fullerene formation from the curved graphene sheets.[26] This model was also recently approved for the some other fused TOC ribbons containing one intermediate benzene ring between each of the TOC fragments.[18] In this way we have predicted that the rectangle 2D sheets like compound **4** can grow and spiralized enough to close the edge vacancies. As a result the new 1D materials are produced in the form of the single-wall nanotubes (Fig. 3, compound **5**). The diameter and length of such type nanotubes depend on the size parameters *a* and *b* of the initial sheet. Another way to modify the size of TOC-based nanotubes is an insertion of the additional benzene rings which enter into the naphthalene-substituted tetraoxa[8]circulene species.[17,24]

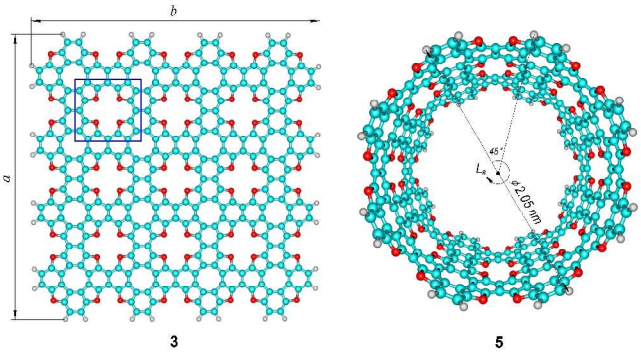

Fig. 3. The optimized structure of the tetraoxa[8]circulene sheet **3** and nanotube **5** both constructed from 16 basic TOC monomers (total side area of compound **5** is equal to 12.0 nm^2).

An important observation is that all tetraoxa[8]circulene sheets **1–4** and nanotubes like **5** contain the 16-crown-4 system[27] (blue square in Fig. 3) which is active in respect to the metal ions extraction[27] (the distance between two opposite Oxygen atoms equals to 4.09 Å). It is possible to compare the 16-crown-4 system with the tetraoxaporphyrin molecule which exists in dicationic form and represents the isoelectronic analogue of diprotonated porphyrin.[28] In this context the studied TOC-based sheets and nanotubes can be compared with the porphyrin sheets (Fig. 1d) described in Ref[15]; the

meso-meso fusion of the four porphyrin molecules produces the central tetraaza[8]circulene core. Similarly, the four tetraoxaporphyrin units surround each TOC unit in the corresponding 2D sheets (Fig. 3). This fact demonstrates the fundamental likeness between the TOC-based and porphyrin-based two-dimensional sheets.

Electronic absorption spectra. Experimental and calculated electronic absorption spectra of the initial tetraoxa[8]circulene compound were previously published and well described.[24a,c] In particular, it was stressed the absence of visible absorption in the observed and calculated UV-vis spectra of the free TOC molecules. Surprisingly, we have found that the tetraoxa[8]circulene sheets **1-4** and nanotube **5** can strongly absorb light in the visible region (around 560 nm, Fig. 4, Table 2) in a great contrast to the free TOC monomer and other π-extended tetraoxa[8]circulenes[17g,h] which demonstrate only weak light absorption near the blue edge of the visible region (below 410 nm).

Table 2. Selected vertical transitions for compounds **1–5**

Compound	State	Transition	λ, nm	M_{xy},[a] a.u	μ_z, β [b]	*f*
1	S_1	$X^1A_{1g}\rightarrow1^1A_{2g}$	519	0	6.22	0.000
	$S_{2(3)}$	$X^1A_{1g}\rightarrow1^1E_u$	482	3.40	0	0.730
	$S_{11(12)}$	$X^1A_{1g}\rightarrow3^1E_u$	382	1.66	0	0.219
2	S_1	$X^1A_{1g}\rightarrow1^1A_{2g}$	592	0	10.69	0.000
	$S_{2(3)}$	$X^1A_{1g}\rightarrow1^1E_u$	561	0.89	0	1.158
3	S_1	$X^1A_{1g}\rightarrow1^1A_{2g}$	635	0	15.62	0.000
	$S_{2(3)}$	$X^1A_{1g}\rightarrow1^1E_u$	610	5.69	0	1.605
	$S_{5(6)}$	$X^1A_{1g}\rightarrow2^1E_u$	576	3.87	0	0.788
4	S_1	$X^1A_g\rightarrow1^1B_{1u}$	562	6.52	0	2.296
	S_6	$X^1A_g\rightarrow2^1B_{2u}$	500	3.47	0	0.732
	S_{11}	$X^1A_g\rightarrow2^1B_{2u}$	459	2.48	0	0.407
	S_{16}	$X^1A_g\rightarrow4^1B_{1u}$	435	2.52	0	0.443
	S_{17}	$X^1A_g\rightarrow5^1B_{1u}$	430	0.39	0	0.150
	S_{25}	$X^1A_g\rightarrow8^1B_{1u}$	408	1.90	0	0.270
	S_{28}	$X^1A_g\rightarrow9^1B_{1u}$	400	2.57	0	0.501
5	S_1	$X^1A_{1g}\rightarrow1^1A_{2g}$	641	0	15.61	0.000
	$S_{2(3)}$	$X^1A_{1g}\rightarrow1^1E_{2u}$	569	5.73	0	1.757

[a] M_{xy} – electric-dipole transition moment in the *xy* molecular plane; [b] β – Bohr magneton.

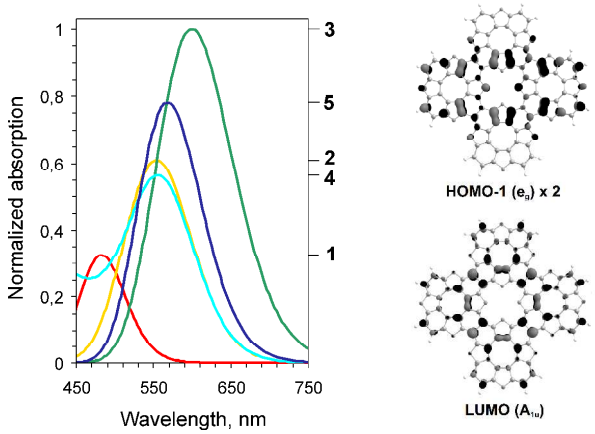

Fig. 4. The calculated electronic absorption spectra (left side) for the compounds **1–5** (the right scale denotes molecular notations corresponding to the absorption peaks) and selected π-MO (right side) for compound **1** illustrating the dibenzofuran chromophore contribution.

In the calculated absorption spectra of the **1–3, 5** species the first electronic transition $X^1A_{1g}\rightarrow1^1A_{2g}$ is symmetry forbidden in the electric-dipole approximation (M_{xy} = 0), but exhibits a large magnetic-dipole transition moment μ_z (Table 2) which increases simultaneously with the total area growth (Table 1). In contrast, the doubly degenerated $X^1A_{1g}\rightarrow{}^1E_u$ electronic transitions (Table 2) are well allowed in the electric-dipole approximation. These transitions are characterized by huge oscillator strength values *f* (Table 2) and determine a strong absorption in the visible region (Fig. 4). It should be noted, that the oscillator strength values are size-depended and qualitatively correlate with the total area parameter (Table 1) of the compounds **1–5** (Table 1). This fact suggests the key role of the π-conjugation effect defining the rice of absorption intensity with the sheet growth. The similar size-depended phenomenon is well reproduced for the 1D TOC ribbons (Fig. 5) presented in Fig. 1f.

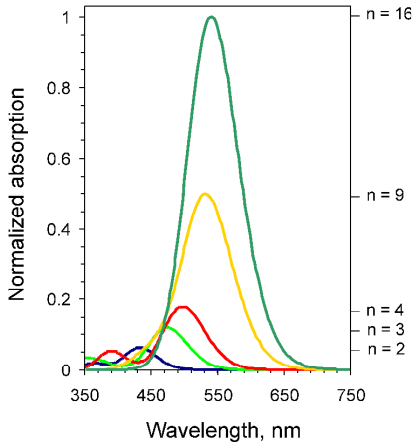

Fig. 5. The calculated electronic absorption spectra for the 1D TOC ribbons (the right scale denotes the ribbon length corresponding to the absorption peaks).

The unusually strong light absorption of the compounds **1–5** can be assigned to formation of cyclic acene chromophores containing naphthalene moieties conjugated with the furan rings. Such acene chromophore can be well observed from the Fig. 4 (right side) containing selected molecular orbitals which form the 1^1E_u excited state of compound **1**. The key role of acene (anthracene) chromophore and its clear manifestation in the absorption spectra were previously demonstrated for the related TOC sheets which contain intermediate epenthetic benzene cores.[18] The MO diagrams and Tables S1, S2 presented in ESI(†) describe additionally the absorption spectra of the **1–5** compounds.

The calculated energy (in the vertical approximation) of the first excited triplet state for compounds **1–5** is about 1.8–2.2 eV, which corresponds to the predicted phosphorescence in the range 570–670 nm (calculated energy of the T_1 exited state monotonously decease when the molecular size increases). The $T_1\rightarrow S_0$ phosphorescence is forbidden by the orbital symmetry selection rule (even with account of spin–orbit coupling effect) and can be induced only by spin-vibronic perturbation. On this background a very weak and long-lived phosphorescence of the studied compound can be predicted.

The HOMO-LUMO gap engineering and charge carrier motilities

The concept of HOMO-LUMO gap (HLG) engineering is very interesting in the context of principal differences between 1D

and 2D materials. This fact opens up new opportunities to create the novel fundamentally different polymers (like TOC sheets and ribbons) based on the same monomers.

The unique electronic coupling in the 1D and 2D TOC-based compounds results in a very strong electronic conjugation, leading to relatively small HLG values. As one can see from the Fig. 6 the HLG evolves as a function of oligomer size (1/n) for both 1D and 2D conjugated structures. It is indicative that the HLG value is contracted by ~1.2 eV in the 1D polymer and by ~2.0 eV in the 2D polymer (n→∞) compared with the initial TOC unit (1/n=1). In this way the principal difference between the 1D and 2D TOC-based conjugated polymers is abundantly clear: at increasing n number the HLG-1/n dependence quenches quickly in the 1D polymers, whereas in the 2D polymers it shows the much more rapid contraction.

One can conclude that the TOC-based 2D sheets are predicted to possess a very low HLG (~1.66 eV at the boundary condition point 1/n = 0) compared with the most of known 2D-conjugated polymers.[8b] The 1D tetraoxa[8]circulene ribbons are also characterized by the significantly low HLG values among the related contestants like phenylene-, tetrathienoanthracene-, triphenylamine-based oligomers and polymers.[8b]

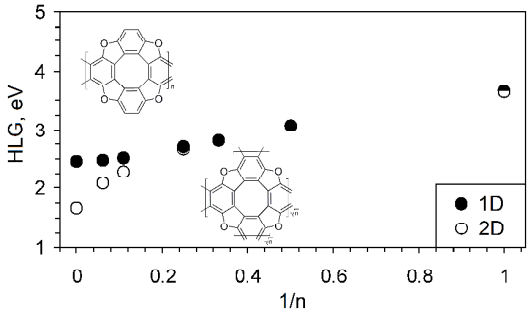

Fig. 6. The size dependence behaviour of HOMO-LUMO gap (HLG) for the TOC-based 1D and 2D oligomers/polymers.

The π-extended TOC-based 2D frameworks **1–4**, 1D ribbons and nanotubes are also predicted to be good electron donors/acceptors which is a general feature of the ambipolar semiconductors.[22] This conclusion has been quantitatively proved on the ground of electron/hole reorganization energies (λ_-/λ_+) calculations by the Eq. 1 (Table 3). One should stress, that the λ_- and λ_+ values show the much more rapid decrease with the rise of n number for the linear 1D oligomers comparing with the corresponding sheets **1–3** (Table 3). This fact demonstrates once again the fundamental size-dependent difference between the 1D and 2D oligomers containing the same number of n-repeating monomers.

Table 3. The cation and anion reorganization energies for the TOC-based oligomers

Compound	n	λ_+, eV	λ_-, eV
1	4	0.045	0.066
2	9	0.042	0.041
3	16	0.032	0.035
4	8	0.055	0.049
1D ribbons	2	0.155	0.115
	3	0.107	0.081
	4	0.066	0.068
	9	0.033	0.032
	16	0.019	0.020
TOC	1	0.203	0.196

The origin of the small cation/anion reorganization energies in the TOC-based oligomers can be understood on the basis of the strong delocalization of unpaired π-electron when the one-electron oxidation/reduction takes place. Moreover, the cationic and anionic oligomers retain the high symmetry without significant deformation of molecular skeleton upon the oxidation/reduction impact. In this way all the terms of Eq. 1 are close similar between each other. This fact provides the small λ_+/λ_- values for the TOC-based materials (Table 3).

Aromaticity of tetraoxa[8]circulene sheets

It is well known that all hetero[8]circulenes(‡) demonstrate an unusual aromatic properties, which are well described by the NICS criterion.[15b,24d,29] The sheets **1–4** are not an exception. Significantly negative NICS(0) and NICS(1) values at the center of the benzene and furane rings for the compound **1** (Fig. 7) indicate the presence of induced diatropic ring current, i.e. aromatic character of these rings.

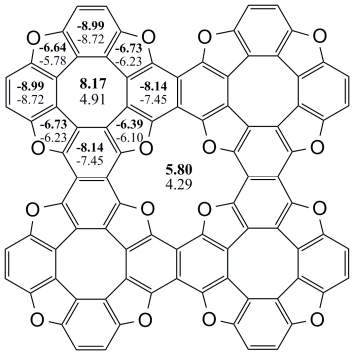

Fig. 7. The NICS(0) (bold type) and NICS(1) (italic type) indexes for the square TOC-based sheet **1**.

The positive NICS(0) and NICS(1) values for the inner cyclooctatetraene and tetraoxaporphyrin cores (Fig. 7) correspond to the presence of the paratropic ring currents, i.e. indicate antiaromaticity of these cores. In this way all studied TOC-based sheets and ribbons are predicted to be nonaromatic compounds because of paratropic and diatropic ring-currents are completely canceled yielding almost zero net current analogously to the well known saturated cyclic hydrocarbons and fullerene C_{60}.[30] In contrast, the dianionic compound **1** is predicted to be completely aromatic species because of the inner cyclooctatetraene, tetraoxaporphyrin cores and all surrounding benzene and furan rings are strongly aromatic (corresponding NICS indexes are significantly negative, Fig. S8, ESI(†)). The dicationic compound **1** is predicted to possess a non-aromatic cyclooctatetraene core, but other benzene, furan rings and tetraoxaporphyrin core support an aromatic character (Fig. S8). Thus, we have predicted that the dicationic sheet **1** in total represents the predominantly aromatic species because of the prevailing diatropic ring currents presence.

Possible routs to synthesize the tetraoxa[8]circulene sheets

The synthesis of the TOC-based sheets and linear oligomers is an extremely important task which would open up the new perspectives to create the novel graphene-like semiconducting materials with the non-zero band-gap. In the present work we have predicted two possible chemical routs to obtain the 2D oligomers **1–4** in accordance with the "bottom-up" principle (from the initial tetraoxa[8]circulene to the objective sheet). The first possible rout represents the intermolecular

dehydrohalogenation (IDHH) process of the corresponding dibromodehydrohelicenes(‡‡) (Scheme 1a). Such reactions are widely used for the C-H bonds functionalization of heteroarenes (these reactions are metal-catalyzed in general).[31]

The calculated enthalpy and the free Gibbs energy for the IDHH schemes 1a and 1b are found to be significantly negative. This fact indicates the principal possibility of these reactions from the thermodynamic point of view though the proposed schemes are hypothetical. The main purpose of the Scheme 1 is to demonstrate the high thermodynamic stability of the TOC-based sheets relative to the initial monomeric units. Indeed, the fusion of the four initial molecules (Scheme 1) provides a formation of the strongly π-conjugated sheet **1** in which the fused bonds (marked by blue colour in Scheme 1) are implicated into the aromatic system of the local naphthalene moiety.

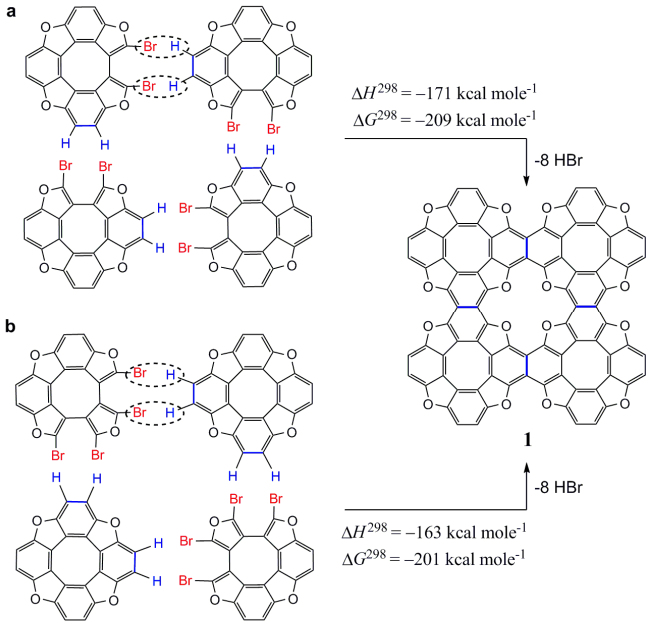

Scheme 1. The intermolecular dehydrohalogenation process as the possible route to synthesize the TOC-based sheet **1**.

The second possible rout represents the Ullman-type polymerization through the tetrabromodehydrohelicenes (Fig. S8) close similar to those presented in Scheme 1. Such rout seems to be very reliable because of the most of presently known 1D and 2D polymers are synthesized through the Ullman-type polymerization.[1c,10c,32] It should be noted that the Ullman polymerization opens up the new routs to synthesize the planar TOC-based 2D frameworks which contain additional four-membered "links" between the coupled monomers (Fig. S8). Such compounds also provide interest for the future investigation.

Conclusions

The nanoscaled 1D ribbons, 2D sheets and single-wall nanotubes containing the directly fused tetraoxa[8]circulene monomers has been designed and described in the present work for the first time. The constructed tetraoxa[8]circulene sheets are found to be absolutely planar compounds which exhibit a trend to the bending ability for a rectangle sheets with the subsequent spiralization and closing into the single-wall nanotube. The designed 1D and 2D compounds are characterized by the strong size-dependent visible absorption because of specific π-conjugation producing the cyclic dibenzofuran chromophore.

Our calculations indicate that the HOMO–LUMO gap of the designed 2D sheets is significantly smaller than that of their linear 1D counterparts at large n values. This fact demonstrates the novel possibilities in the "band-gap engineering" activity which is booming nowadays in order to create new materials for the molecular organic electronics. Indeed, all designed compounds (except initial tetraoxa[8]circulene monomer) are predicted to be ambipolar organic semiconductors. This prediction is supported by the very small values of the electrone/hole reorganization energies.

In the present work we have additionally predicted the possible ways for the experimental synthesis of the designed compounds. Among all considered reaction schemes only two routs seem to be the most reliable from the thermodynamic point of view: (i) the intermolecular metal-catalyzed dehydrohalogenation and (ii) the Ullman-type polymerization widely used nowadays for the synthesis of new 1D and 2D π-conjugated materials.

Calculations with the small and large basis sets for the smallest square molecule **1** justify the reliable accuracy level of the methods used and all conclusions remain. For instance, the deviations in the bond lengths calculated with the two different basis sets 6-21G(d) and 6-31G(d) are negligibly small and do not exceed 0.004 Å. The estimated HGL values are equal to 2.69 and 2.72 eV, respectively, which indicates also the close similarity of both approaches. As a general tendency,[8b] the combination of the B3LYP functional and the 6-31G(d) basis set (which is similarly predicts the structure, λ_+/λ_- and HLG values comparing with the 6-21G(d) basis set) is a reasonably well approach to predict the HLG of organic polymers[35] and seems to circumnavigate the frequently encountered underestimation of the band gap for the 3D metals and semiconductors.[36]

Acknowledgements

All computations are performed with resources provided by the Swedish National Infrastructure for Computing (SNIC) at the Parallel Computer Center (PDC) through the project "Multiphysics Modeling of Molecular Materials", SNIC 020/11-23. This research was also supported by the Ministry of Education and Science of Ukraine (project number 0113U001694).

Notes and references

[a] *Bohdan Khmelnytsky National University, Cherkassy, 18031, Ukraine. E-mail: glebchem@rambler.ru, bfmin@rambler.ru*
[b] *Tomsk State University, 634050, Tomsk, Russian Federation*

† Electronic Supplementary Information (ESI) available: bond lengths for S_0 and T_1 states of compound **1**, optimized Cartesian coordinates for compounds **1–5** and linear oligomers (n=2–4,9,16), MOs energy diagrams for compounds **1–5,** NICS calculations for the dicationic and dianionic compound **1**, chemical schemes of the Ullman-type polymerization for the synthesis of compound **1**. See DOI: 10.1039/b000000x/

‡ The hetero[8]circulenes family includes already synthesized tetraoxa[8]circulenes, azaoxa[8]circulenes, thio[8]circulenes and numerous theoretically predicted hetero[8]circulenes, containing different types of heteroatoms and groups (B, N, P, As, BF_2, AlF_2, GaF_2 etc.)[29a,b,d,33]

‡‡ Compounds (such as the reagents in Scheme 1a) in which the two helical termini of a helicene are connected by a σ-bond are called dehydrohelicenes. The sulfuric dehydrohelicenes were synthesized and comprehensively studied by the H. Wynberg and colleagues.[34] The proposed oxygen-containing dibromodehydrohelicenes are not synthesized yet whereas they are closing similar to the sulfuric analogs and related polythioles.[33a]

1 a) J. R. Heath and M. A. Ratner, *Physics Today*, 2003, **56**, 43; b) L. Bartels *Nat. Chem.*, 2010, **2**, 87; c) S. W. Hla, L. Bartels, G. Meyer and K.-H. Rieder, *Phys. Rev. Lett.*, 2000, **85**, 2777.

2 a) B. Minaev, G. Baryshnikov and H. Agren, *Phys. Chem. Chem. Phys.*, 2014, **16**, 1719; b) Y. Tao, C. Yang and J. Qin, *Chem. Soc. Rev.*, 2011, **40**, 2943.

3 a) K. S. Novoselov, A. K. Geim, S. V. Morozov, D. Jiang, Y. Zhang, S. V. Dubonos, I. V. Grigonrieva and A. A. Firsov, *Science*, 2004, **306**, 666; b) Geim A. K. and Novoselov K. S., *Nat. Mater.* 2007, 6, 183.

4 a) X.-H. Liu, C.-Z. Guan, D. Wang and L.-J. Wan, *Adv. Mater.*, 2014, DOI: 10.1002/adma.201305317; b) M. Xu, T. Liang, M. Shi and H. Chen, *Chem. Rev.*, 2013, **113**, 3766; c) T. Govindaraju and M. B. Avinasha, *Nanoscale*, 2012, **4**, 6102. d) Y. Lin and J. W. Connell, *Nanoscale*, 2012, **4**, 6908; e) R. Mas-Balleste, C. Gomez-Navarro, J. Gomez-Herrero and F. Zamora, *Nanoscale*, 2011, **3**, 20; f) Q. Tang, Z. Zhou, *Prog. Mater. Sci.*, 2013, **58** 1244.

5 S. Perumal, B. Minaev and H. Ågren, *J. Chem. Phys.*, **136**, 104702.

6 a) J. Bai, X. Zhong, S. Jiang, Y. Huang and X. Duan, *Nat. Nanotechnol.* 2010, **5**, 190; b) L. Jiang and Z. Fan, *Nanoscale*, 2014, **6**, 1922.

7 J. Nisar, X. Jiang, B. Pathak, J. Zhao, T. W. Kang and R. Ahuja *Nanotechnology*, 2012, **23**, 385704.

8 a) J. Sakamoto, J. v. Heijst, O. Lukin and A. D. Schluter, *Angew. Chem. Int. Ed.*, 2009, **48**, 1030; b) R. Gutzler and D. F Perepichka, *J. Am. Chem. Soc.*, 2013, **135**, 16585; c) D.F. Perepichka and F. Rosei, *Science*, 2009, **323**, 216.

9 C.-A. Palma and P. Samorì, *Nat. Chem.*, 2011, **3**, 431.

10 a) L. Grill, M. Dyer, L. Lafferentz, M. Persson, M. V. Peters and S. Hecht, *Nat. nanotechnol.*, 2007, **2**, 687; b) L. Lafferentz, V. Eberhardt, C. Dri, C. Africh, G. Comelli, F. Esch, S. Hecht and L. Grill *Nat. Chem.*, 2012, **4**, 215; c) A. Gourdon *Angew. Chem. Int. Ed.*, 2008, **47**, 6950; d) R. Gutzler, H. Walch, G. Eder, S. Kloft, W. M. Hecklab and M. Lackinger, *Chem. Commun.*, 2009, 4456; e) L. Cardenas, R. Gutzler, J. Lipton-Duffin, C. Fu, J. L. Brusso, L. E. Dinca, M. Vondracek, Y. Fagot-Revurat, D. Malterre, F. Rosei and D. F. Perepichka, *Chem. Sci.*, 2013, **4**, 3263; f) M. Matena, T. Riehm, M. Stöhr, T. A. Jung and L. H. Gade, *Angew. Chem. Int. Ed.*, 2008, **47**, 2414.

11 Y. Li, J. Xiao, T. E. Shubina, M. Chen, Z. Shi, M. Schmid, H.-P. Steinruck, J. M. Gottfried, and N. Lin, *J. Am. Chem. Soc.* 2012, **134**, 6401.

12 S. A. Krasnikov, C. M. Doyle, N. N. Sergeeva, A. B. Preobrajenski, N. A. Vinogradov, Y. N. Sergeeva, A. A. Zakharov, M. O. Senge and A. A. Cafolla, *Nano Res.*, 2011, **4**, 376.

13 a) M. Abel, S. Clair, O. Ourdjini, M. Mossoyan and L. Porte *J. Am. Chem. Soc.*, 2011, **133**, 1203; b) J. Zhou and Q. Sun, *J. Am. Chem. Soc.,* 2011, **133**, 15113.

14 E. L. Spitler and W. R. Dichtel, *Nat. Chem.*, 2010, **2**, 672.

15 a) Y. Nakamura, N. Aratani, K. Furukawa and A. Osuka, *Tetrahedron*, 2008, **64**, 11433. b) Y. Nakamura, N. Aratani, H. Shinokubo, A. Takagi, T. Kawai, T. Matsumoto, Z. S. Yoon, D. Y. Kim, T. K. Ahn, D. Kim, A. Muranaka, N. Kobayashi and A. Osuka, *J. Am. Chem. Soc.*, 2006, **128**, 4119.

16 a) A. Tsuda, H. Furuta and A. Osuka, *Angew. Chem. Int. Ed.* 2000, **39**, 2549; b) A. Tsuda and A. Osuka, *Science*, 2001, **293**, 79.

17 a) H. Erdtman and H.-E. Högberg, *Chem. Commun.,* 1968, 773; b) H. Erdtman and H.-E. Högberg, *Tetrahedron Lett.*, 1970, **11**, 3389; c) H.-E. Högberg, *Acta Chem. Scand.*, 1972, **26**, 309; d) H.-E. Högberg, *Acta Chem. Scand.*, 1972, **26**, 2752. e) H.-E. Högberg, *Acta Chem. Scand.*, 1973, **27**, 2559. f) H.-E. Högberg, *Acta Chem. Scand.*, 1973, **27**, 2591. g) J. Eskildsen, T. Reenberg and J. B. Christensen, *Eur. J. Org. Chem.*, 2000, 1637; h) C. B. Nielsen, T. Brock-Nannestad, T. K. Reenberg, P. Hammershoj, J. B. Christensen, J. W. Stouwdam and M. Pittelkow, *Chem. Eur. J.*, 2010, **16**, 13030.

18 G. V. Baryshnikov, B. F. Minaev, N. N. Karausha and V. A. Minaeva, *Phys.Chem.Chem.Phys.*, 2014, **16**, 6555.

19 a) A. D. Becke, *J. Chem. Phys.*, 1993, **98**, 5648; b) C. Lee, W. Yang and R. G. Parr, *Phys. Rev. B.*, 1988, **37**, 785; c) M. S. Gordon, J. S. Binkley, J. A. Pople, W. J. Pietro and W. J. Hehre, *J. Am. Chem. Soc.*, 1982, **104**, 2797; d) M. M. Francl, W. J. Pietro, W. J. Hehre, J. S. Binkley, D. J. DeFrees, J. A. Pople and M. S. Gordon, *J. Chem. Phys.*, 1982, **77**, 3654. d) R. Krishnan, J. S. Binkley, R. Seeger and J. A. Pople, *J. Chem. Phys.*, 1980, **72**, 650.

20 M. J. Frisch, G. W. Trucks, H. B. Schlegel, G. E. Scuseria, M. A. Robb, J. R. Cheeseman, G. Scalmani, V. Barone, B. Mennucci, G. A. Petersson, H. Nakatsuji, M. Caricato, X. Li, H. P. Hratchian, A. F. Izmaylov, J. Bloino, G. Zheng, J. L. Sonnenberg, M. Hada, M. Ehara, K. Toyota, R. Fukuda, J. Hasegawa, M. Ishida, T. Nakajima, Y. Honda, O. Kitao, H. Nakai, T. Vreven, J. A. Montgomery, Jr., J. E. Peralta, F. Ogliaro, M. Bearpark, J. J. Heyd, E. Brothers, K. N. Kudin, V. N. Staroverov, R. Kobayashi, J. Normand, K. Raghavachari, A. Rendell, J. C. Burant, S. S. Iyengar, J. Tomasi, M. Cossi, N. Rega, J. M. Millam, M. Klene, J. E. Knox, J. B. Cross, V. Bakken, C. Adamo, J. Jaramillo, R. Gomperts, R. E. Stratmann, O. Yazyev, A. J. Austin, R. Cammi, C. Pomelli, J. W. Ochterski, R. L. Martin, K. Morokuma, V. G. Zakrzewski, G. A. Voth, P. Salvador, J. J. Dannenberg, S. Dapprich, A. D. Daniels, Ö. Farkas, J. B. Foresman, J. V. Ortiz, J. Cioslowski and D. J. Fox, *Gaussian 09, revision C.02*, Gaussian, Inc., Wallingford, CT, 2009.

21 E. Runge and E. K. U. Gross, *Phys. Rev. Lett.*, 1984, **52**, 997.

22 a) A. Datta, S. Mohakud and S. K. Pati, *J. Chem. Phys.*, 2007, **126**, 144710; b) A. Datta, S. Mohakud and S. K. Pati, *J. Mater. Chem.*, 2007, **17**, 1933; c) V. Mohan and A. Datta, *J. Phys. Chem. Lett.*, 2010, **1**, 136; d) S. Mohakud and S. K. Pati, *J. Mater. Chem.*, 2009, **19**, 4356.

23 a) P. v. R. Schleyer, *Chem. Rev.*, 2001, **101**, 1116; b) Z. Chen, C. S. Wannere, C. Corminboeuf, R. Puchta, and P. v. R. Schleyer, *Chem. Rev.,* 2005, **105**, 3842.

24 a) B. F. Minaev, G. V. Baryshnikov, V. A. Minaeva, *Comp. Theor. Chem.*, 2011, **972**, 68; b) A. Minaeva, B. F. Minaev, G. V. Baryshnikov, H. Agren and M. Pittelkow, *Vib. Spectrosc.*, 2012, **61**, 156; c) N. N. Karaush, B. F. Minaev, G. V. Baryshnikov and V. A. Minaeva, 2014, **116**, 33. d) G. V. Baryshnikov, B. F. Minaev, M. Pittelkow, C. B. Nielsen and R. Salcedo, *J. Mol. Model.*, 2013, **19**, 847;

25 P. B.Karadakov, *J. Phys. Chem. A,* 2008, **112**, 12707.

26 H. W. Kroto and K. McKay, *Nature*, 1988, **331**, 328.

27 a) Y. Inoue, T. Hakushi, Y. Liu and L. H. Tong, *J. Org. Chem.*, 1993, **58**, 5411; b) J. K. Park, *J. Phys. Chem. A*, 2002, **106**, 3008.

28 a) E. Vogel, W. Haas, B. Knipp, J. Lex and H. Schmickler, *Angew. Chem. Int. Ed.*, 1988, **27**, 406–409; b) I. Jelovica, L. Moroni, C. Gellini, P. R. Salvi and N. Orlić, *J. Phys. Chem. A*, 2005, **109**, 9935.

29 a) C. V. Nielsen, T. Brock-Nannestad, P. Hammershøj, T. K. Reenberg, M. Schau-Magnussen, D. Trpcevski, T. Hensel, R. Salcedo, G. V. Baryshnikov, B. F. Minaev and M. Pittelkow, *Chem. Eur. J.*, 2013, **19**, 3898; b) T. Hensel, D. Trpcevski, C. Lind, R. Grosjean, P. Hammershøj, C. V. Nielsen, T. Brock-Nannestad, B. E. Nielsen, M. Schau-Magnussen, B. Minaev, G. V. Baryshnikov and M. Pittelkow, *Chem. Eur. J.*, 2013, **19**, 17097; c) S. Radenković, I. Gutman and P. Bultinck, *J. Phys. Chem. A.*, 2012, **116**, 9421; d) T. Ohmae, T. Nishinaga, M. Wu and M. Iyoda, *J. Am. Chem. Soc.*, 2010, **132**, 1066.

30 H. Fliegl, S. Taubert, O. Lehtonen and D. Sundholm, *Phys. Chem. Chem. Phys.*, 2011, **13**, 20500.

31 R. Rossi, F. Bellina, M. Lessi and C. Manzinia, *Adv. Synth. Catal.*, 2014, **356**, 17.

32 a) R. Gutzler, L. Cardenas, J. Lipton-Duffin, M. El Garah, L. E. Dinca, C. E. Szakacs, C. Fu, M. Gallagher, M. Vondráček, M. Rybachuk, D. F. Perepichka, F. Rosei, *Nanoscale* **2014**, 6, 2660; b) F. Schlutter, T. Nishiuchi, V. Enkelmann and K. Mullen, *Angew. Chem. Int. Ed.*, 2014, **53**, 1538–1542.

33 a) K. Yu. Chernichenko, V. V. Sumerin, R. V. Shpanchenko, E. S. Balenkova and V. G. Nenajdenko, *Angew. Chem. Int. Ed.*, 2006, **45**, 7367; b) A. Dadvand, F. Cicoira, K. Yu. Chernichenko, E. S. Balenkova, R. M. Osuna, F. Rosei and V. G. Nenajdenko, *Chem. Commun.*, 2008, 5354. c) T. N. Gribanova, N. S. Zefirov and V. I. Minkin, *Pure Appl. Chem.*, 2010, **82**, 1011; d) G. Gahungu, J. Zhang, *Phys. Chem. Chem. Phys.*, 2008, **10**, 1743; e) T. N. Gribanova, N. S. Zefirov and V. I. Minkin, *Doklady Chem.*, 2009, **426**, 105; f) T. B. Tai, V. T. T. Huong and M. T. Nguyen, *Chem. Commun.*, 2013, **49**, 11548; g) L.-W. Shi, B. Chen, J.-H. Zhou, T. Zhang, Q. Kang an M.-B. Chen, *J. Phys. Chem. A.*, 2008, **112**, 11724.

34 a) M. B. Groen, H. Schadenberg, H. Wynberg, *J. Org. Chem.*, 1971, **36**, 2797; b) J. H. Dopper, D. Oudman, H. Wynberg, *J. Am. Chem. Soc.*, 1973, **95**, 3692; c) J. H. Dopper, D. Oudman, H. Wynberg, *J. Org. Chem.*, 1975, **40**, 3398.

35 S. S. Zade, N. Zamoshchik, M. Bendikov, *Acc. Chem. Res.*, 2010, **44**, 14.

36 H. Xiao, J. Tahir-Kheli, W. A. Goddard III, *J. Phys. Chem. Lett.*, 2011, **2**, 212.

